



RUTIN AND BERBERINE LOADED EUDRAGIT NANOPARTICLES USED IN CANCER TREATMENT: FORMULATION, OPTIMIZATION, AND INVITRO CYTOTOXICITY ACTIVITY

Padmavathy J¹, Sathesh Kumar S^{2*}

Article History:

Received: 01.02.2023

Revised: 07.03.2023

Accepted: 10.04.2023

Abstract

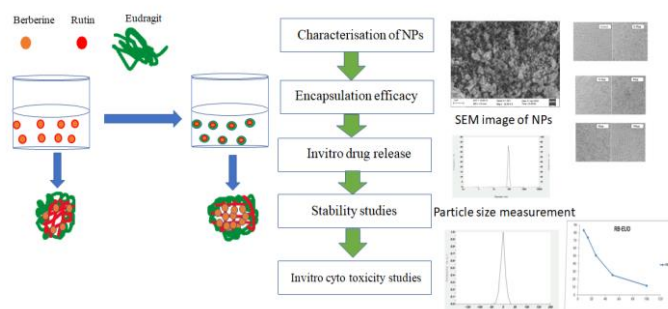
Objective: The present study aims to prepare and improve polymeric nanoparticles for rutin and berberine site-specific delivery in cancer treatment. Eudragit, a pH-sensitive polymer used in the formulation of the nanoparticles, was used to achieve site-specific distribution.

Materials and methods: Nanoparticles were prepared by using ionic gelation method. For formulation optimization and validation, the central composite design has been used. SEM micrographs, nanoparticle size analysis, zeta potential analysis by DLS, encapsulation effectiveness, *in-vitro* drug release profile, and stability were all the parameters evaluated for the optimized formulation.

Results: The characterization results showed that the nanoparticles' surfaces were smooth, and the particle size was determined to be 101.4 nm. Zeta potential was determined to be -0.98 ± 0.05 mV and encapsulation efficiency to be 92.96% for rutin and 96.96% for berberine, respectively. Rutin and berberine-loaded nanoparticles (RB-NPs) were found to be cytotoxic when tested *in-vitro* on the EAC (Ehrlich-Lettre Ascites-E) cell line. Rutin and berberine-loaded NPs were shown to have a percentage cell viability of 83.09% and 6.25%, respectively.

Conclusion: According to the study's findings, it is possible to successfully encapsulate hydrophobic herbal compounds like rutin and berberine, which have clear anti-cancer potential, in a nanoparticulate system to increase its therapeutic effectiveness and site-specific delivery.

GRAPHICAL ABSTRACT



Keywords: - Berberine, Rutin, Eudragit, nanoparticles, MTT assay, EAC cell line

¹Department of Pharmaceutics, School of Pharmaceutical Sciences, Vels Institute of Science, technology and Advanced Studies (VISTAS), Chennai, Tamilnadu, India.

^{2*}Head of the Department & Professor, Department of Pharmaceutics, School of Pharmaceutical Sciences, Vels Institute of Science, Technology and Advanced Studies(VISTAS), Pallavaram, Chennai, Tamil Nadu, India – 600043. Mail Id: sathesh2000@gmail.com

*Corresponding Author: - Dr. S. Sathesh Kumar

* Head of the Department & Professor, Department of Pharmaceutics, School of Pharmaceutical Sciences, Vels Institute of Science, Technology and Advanced Studies(VISTAS), Pallavaram, Chennai, Tamil Nadu, India – 600043,

E-Mail Id: sathesh2000@gmail.com

DOI: - 10.48047/ecb/2023.12.4.263

INTRODUCTION

One of the world's deadliest diseases, cancer results in the deaths of tens of hundreds to millions around the world each year. In the latter half of the 20th century, cancer was the most common and dangerous medical ailment worldwide¹. One of the most problematic aspects of cancer treatment is the capacity to distinguish between cancerous and normal cells in the human body or organs². For instance, radio therapy and other cancer treatments are currently unable to target malignant cells selectively without hurting healthy cells; the main objective of therapeutic research was to detect diseased cells and stop them from proliferating. Cancer therapy and the development of efficient medicines to combat it are hindered by a number of factors, such as wrong medication dosage, adverse side effects from improper drug distribution in tissues, and tumor cells' ability to resist chemotherapy³⁻⁷. The field of research of nanotechnology is distinct and evolving with cutting-edge technology⁸⁻⁹. The development of a reliable, non-toxic, and effective nanoparticle synthesis technique is required since nano technology is developing as a multi functional technology but is limited in clinical research due to the use of dangerous compounds in nano particle synthesis^{10,11}. Nanoparticles are being created and used as prognostic indicators to treat cancer and enhance dosage formulations for specific medications. Proteins, peptides, and bioflavonoids can be delivered in a variety of pharmacological dose forms using polymeric-based nanoparticles^{12,13}. They offer regulated drug delivery of encapsulated hydrophobic molecules at the target site, are more stable, and have a greater encapsulation efficiency, all of which improve bioavailability^{14,15}. The potency of herbal anti-cancer medicines in preventing and treating cancer is also receiving attention. Many herbal medicines are being tested for their ability to fight cancer, but many have poor aqueous solubility, poor absorption, and negligible therapeutic efficacy^{16,17}.

According to reports in the literature, various researchers have successfully shown how encapsulating herbal medications in a lipid nano particle system improves their therapeutic efficacy¹⁸⁻²². Herbal remedies with well-established anti-cancer activity for treatment include rutin and berberine. Rutin and berberine don't target malignant cells at specific sites, have poor water solubility, and have low bioavailability. To create site-specific polymeric

nanoparticles for cancer treatment, rutin and berberine were used as model bioactive agents^{23,24}. The current study aims to use the pH-sensitive polymer eudragit to create site-specific polymeric nanoparticles that contain rutin and berberine. Since eudragit is insoluble in the stomach's acidic medium, it improves drug distribution to the distal section of the gastrointestinal tract, enhancing the therapeutic effect of the anti-cancer agent²⁵. A systemic analytical tool to ascertain the impact of the response variables and the interaction between the independent factors is the design of experiments (DOE). D-optimal, central composite and Behnken are commonly employed response surface techniques for designing experiments^{26,27}. Optimize the formulation of the polymer nanoparticulate in the current investigation using the Central Composite design. The prepared nanoparticles were further subjected to physicochemical analysis qualities, study of drug content, drug release profile, and stability study.

MATERIALS AND METHOD

Eudragit, degree of deacetylation: ~75 %, SRL chemicals India was used as a starting material. Rutin and Berberine were purchased from Sigma Aldrich, India. Sodium tripolyphosphate (TPP, Sigma Aldrich, India), Glacial acetic acid (Qualigens), Ethanol (95% china make) were used in nanoparticle preparation. Millipore water was used in this study.

Preparation of rutin and berberine-loaded eudragit nanoparticles (Ionic gelation method)

Eudragit was dissolved in 1% acetic acid with stirring overnight. Sodium hydroxide (2M) solution was used to change the pH of the solution to 4.7. A 0.45 m filter has been used to filter the eudragit solution. Rutin (50mg) and Berberine (50mg) were dissolved in 5ml ethanol and added into 30 ml of Eudragit solution under magnetic stirring. Then, as a cross-linking agent, 15ml of TPP solution was introduced in drops to the RB-CS solution and mixed at various rates. Subsequently, the non-entrapped drug and dissolved Eudragit were extracted using a chilled centrifuge at 12,000 rpm for 20 minutes, and the nanoparticles were freeze-dried and stored in a vacuum desiccator^{28,29}.

Drug-loaded eudragit nanoparticles optimization

The formulation of rutin and berberine-loaded nanoparticles was Central Composite experimental design optimization is achieved using Design expert software 11 3-factor, 3-level

(Test Version) with 17 developed formulas. Table 1 summarises the chosen variables and responses. The conversation Polynomial analysis was done between the variables. Equations and response surface visualizations in three dimensions Design-Expert® Software 11 generated Central Composite design's creation of a polynomial equation as shown by the following equation.

$$Y=A_0+A_1*X_1+A_2*X_2+A_3*X_3+A_4*X_4+A_5*X_1*X_2+A_6*X_1*X_3+A_7*X_1*X_4+A_8*X_2*X_3+A_9*X_2*X_4+A_{10}*X_3*X_4+A_{11}*X_1^2+A_{12}*X_2^2+A_{13}*X_3^2+A_{14}*X_4^2+A_{15}*X_1*X_2+A_{16}*X_1*X_3+A_{17}*X_1*X_4$$

Where A1 to A17 have predicted values, X1 through X4 are coded variables for independent factors, Y is the response coefficient of determination variables, and A0 is the intercept. Xa, Xb (where in there a and b are 1,2,3,4), and Xi (where I was 1,2,3,4) represent interaction terms. The independent variable's impact on particle diameter, surface charge, and encapsulation efficiency was indicated by the desirable and undesirable signs to the magnitude of the parameters in the quadratic function. The highest encapsulation effectiveness and smallest particle size were the qualifying criteria for the optimized formulation.

Characterization of rutin and berberine loaded eudragit nano particles

Scanning electron microscope

The prepared nanoparticles' morphology characteristics were analyzed using scanning electron microscopy (SEM) (SEM; JEOL JMS-6390 apparatus). The samples were coated with carbon to increase electron beam conductivity. A raster of signals produced by an electron beam that enters a sample of nanoparticles provides information about the sample morphology and other features.

Zeta potential analysis

In a Nanoparticle size analyzer with a maximum output of 4mW and measurement accuracy of 0.12m/Vs, When measuring the surface charge of aqueous systems, NISTSRM1980 reference standard material was used. The Henry equation was used in the Zeta Potential series to calculate the zeta potential after determining the particle surface.

$$UE=2\epsilon(ka)/3\eta$$

Where is the Zeta potential, the dielectric constant, surface charge, Henry function, medium's absolute zero-shear viscosity, and particle radius to Debye length ratio. Electrophoretic mobility is the term used to describe a particle's motion in an electric field. A little amount of colloidal suspension was used to analyze the material in quartz cuvettes. The standard deviation and zeta potential were reported.

2.3.3 Encapsulation Efficacy

The encapsulation effectiveness of the RB-ES-NPs was determined by using UV-visible (UV) spectrophotometric analysis. About 10 mg of nano particles were accurately weighed and dissolved using Methanol (10ml). After that, the solutions were agitated at 8000 rpm for 15 mins. The solution was filtered, and a 420nm wave length was used to measure the drug concentration in the supernatant at room temperature. The following calculation was used to calculate the percentage of medication encapsulated:

$$\text{Encapsulation efficiency (\%)} = \frac{\text{Total Weight of drug-Free drug weight}}{\text{Total weight of drug}} \times 100$$

Determination of drug content of nanoparticles

By removing the drug from the RB-NPS nanoparticles, the effectiveness of the drug loading was assessed. 50 mg of nanoparticles were added to 100 ml of 10% HCl, which was maintained at roughly 35°C for 24 hours. After that, the drug concentration in the liquid supernatant was determined, and the nanoparticles were centrifuged at 8000 rpm. A similar process was used to assess unloaded nanoparticles. It was calculated how much drug would be loaded. Three duplicates of the experiment were performed, and the mean results were recorded.

$$\text{Drug content (\%)} = \frac{\text{Amount of drug in nanoparticles} \times 100}{\text{Amount of nanoparticles}}$$

Invitro drug release study of rutin and berberine loaded eudragit nanoparticles

In terms of determining the drug release by in vitro drug release study, the RB-ES-NP, phosphate buffers with pH values of 6.8, 7.4, and hydrochloric acid with a pH of 1.2 were utilized. The dissolving media containing the NPs (10mg) was heated to 37°C while magnetic stirring was used to maintain ideal sink conditions. At certain intervals, the same amount of fresh medium was inserted after the samples were removed. UV spectrophotometric analysis was used to determine how much medication was present in the supernatant after samples were

centrifuged the samples at 8000 rpm for five minutes.

Invitro cytotoxicity study (MTT assay)

The MTT test was used to determine an *in vitro* cytotoxicity research. EAC (Ehrlich-Lette Ascites -E) cell line was utilized. The 96-well plates with Roswell Park Memorial Institute Medium (RPMI) 1640, 10% fetal calf serum (FCS), and $5\% \pm 0.5\text{CO}_2$ at $37^\circ\text{C} \pm 0.05$. Cells were treated with RB-NPs at five different concentrations: 6.25 $\mu\text{g}/\text{ml}$, 12.5 $\mu\text{g}/\text{ml}$, 25 $\mu\text{g}/\text{ml}$, 50 $\mu\text{g}/\text{ml}$, and 100 $\mu\text{g}/\text{ml}$. All samples have a DMSO concentration of less than 0.1 percent. The MTT reagents were present in all cells, and they were keeping it for 4 hours. In a safety cabinet, the cells' deep blue formazan product was created. After that, it was dissolved in a DMSO solution, and a plate reader was used to detect the absorbance at 550 nm. The following formula was used to determine the viability percentage: $\text{Sample abs}/\text{Control abs} \times 100 = \text{percentage of viability}$.

Stability study

The samples of the RB-ES-NP formulation were tested for stability during 180 days periods at temperatures between 2 and 8 $^\circ\text{C}$. The samples were taken out and tested for particle size, zeta potential, and encapsulation effectiveness after intervals of 30, 90, and 180 days.

RESULT AND DISCUSSION

Experimental design for optimization of rutin and berberine loaded eudragit nanoparticles

The observations of the corresponding response variables for each of the seventeen nanoparticle formulations created using the Design Expert® software Table 2 summarizes the results. The information found was suited to mathematical models from 17 formulations. Employing models such as linear, first-order, cubic, and quadratic to research interaction, use Design Expert® Software 11 involving the variables; the experimental strategy showed the best model that fits RB-ENPS is the quadratic one. Analysis of NPs Plots of three-dimensional graphs was made to research the effects of each answer.

Particle size (Y1)

The following is the quadratic equation created for the Y1 response for RB-E-NPs:
$$Y1 = +98 + 84.50X1 + 16.12X2 - 70.13X3 - 32.00X1X2 - 13.00X1X3 - 41.75X2X3 + 106.63X1^2 + 108.88X2^2 + 27.37X3^2$$

According to the ANOVA analysis, significant model terms are provided for response Y1 by the independent variables and their interaction effects for reaction; Y1 was discovered to be less than 0.0001 (Table 3). The values of adjusted R^2 , predicted R^2 , and sequential P-value for particle size of nanoparticles (Y1), zeta potential (Y2), and encapsulation effectiveness of berberine and rutin (Y3 and Y4) shows in table 4.

The quadratic equation indicates that the volume of eudragit (X1) and volume of the organic phase (X3) have a favorable impact on particle size. Due to the enormous volume of the medium present, the volume has increased, which may be the cause of the increase in particle size. The particle size gradually grew as quantity increased in the RBE-NPS of drug loading. Surfactant, however, (X2) demonstrated a reduction in NPs' particle size after an increase in concentration brought on by the emergence of small droplets. These are the three-dimensional response graphs (Figs. 1a, 1b, and 1c).

Zeta potential (Y2)

The following is the quadratic equation created for the Y2 response for RB-E-NPs:

$$Y2 = -1.20 - 0.6437X1 - 0.4462X2 + 0.4650 - 0.8075X3 - 0.5700X1X2 + 0.3400X1X3 - 0.5163X2X3 - 0.5163X1^2 + 0.3238X2^2 - 1.21X3^2$$

According to the results of the ANOVA analysis, significant model terms are provided for response Y2 by the independent variables and their interaction effects. The P-value for response Y2 was determined to be 0.0486 (Table 5).

According to the quadratic equation above, the volume of the organic phase (X3) and the volume of the eudragit (X1) have a synergistic influence on the response Y2. The zeta potential of the nanoparticles did, however, decrease at greater surfactant concentrations. Figs. 2a, 2b, and 2c depict the three-dimensional response graphs for Y2.

Encapsulation efficacy of berberine (Y3)

The following is the quadratic equation created for the Y3 response for RB-E-NPs:

$$Y3 = +91.00 - 5.50X1 - 6.62X2 - 0.6250X3 + 2.50X1X2 + 12.50X1X3 + 7.25X2X3 - 29.13X1^2 + 0.6250X2^2 - 0.3750X3^2$$

According to the results of the ANOVA analysis, significant model terms are provided for response

Y3 by the independent variables and their interaction effects. The P-value for response Y3 was determined to be 0.0041 (Table 6).

Eudragit (X1) and volume of the organic phase (X3) have a synergistic effect on reaction Y3, as shown by the quadratic equation above. However, the increased concentration of surfactant exhibited a decline in the encapsulation efficiency of berberine. Figs. 4a, 4b, and 4c illustrate the three-dimensional response graphs (Y3).

Encapsulation efficacy of rutin(Y4)

The following is the quadratic equation created for the Y4 response of RB-E-NPS:

$$Y4 = +96.00 - 8.25X1 + 1.50X2 + 5.00X3 - 5.00X1X2 - 1.00X1X3 - 13.00X2X3 - 12.75X1^2 - 8.25X2^2 - 8.75X3^2$$

According to the results of the ANOVA analysis, significant model terms are provided for response Y4 by the independent variables and their interaction effects. The P-value for response Y4 was determined to be 0.0142 (Table 7).

Eudragit (X1) and volume of the organic phase (X3) have a synergistic effect on reaction Y3 as shown by the quadratic equation above. However, the increased concentration of surfactant exhibited a decline in the encapsulation efficiency of berberine. Figs. 3a, 3b, and 3c illustrate the three-dimensional response graphs (Y4).

Optimization and validation

Using the Design-Expert software numerical point prediction method, the optimal formulation of RB-E-NPs was chosen based on the criteria of achieving the minimum possible particle size and the highest possible encapsulation effectiveness. The chosen optimized formulation for RBE-NPs constituted 100% organic phase solution, 10% polyvinyl alcohol, and 6% eudragit polymer, with a desirability value of 0.954. The experimentally determined particle size (101.4 nm), zeta potential (-0.98 mV) and berberine and rutin entrapment efficiency (96.96% and 92.96%) of RBE-NPs were found to be consistent with the projected particle size value (122 nm), zeta potential (-0.96 mV) and berberine and rutin entrapment efficiency (99% and 82%) produced by Design expert software.

Characterization of drug-loaded eudragit nanoparticles

Using SEM, the optimized nanoparticles displayed a spherical shape (Fig. 5). It was discovered that nanoparticles have an average

particle size of 101.4 nm (Fig. 6). Fig. 7 depicts the particle size distribution for optimized RBE-NPs. Zeta and the polydispersity index potential was measured at -0.98 mV, respectively. The low polydispersity index value and Zeta potential's negative value support the uniform particle dispersion and strong physical stability of the delivery mechanism. The efficiency of encapsulation was 92.96 and 96.96% were calculated to be the results.

Drug content (%) of drug-loaded nanoparticles

The results of the berberine and rutin-loaded nanoparticles' calculated drug content are 99.86 and 99.70%. Then nanoparticles contained the highest amount of medication content.

Drug release in vitro study of nanoparticles with rutin and berberine

In vitro drug profile (Fig. 8) shows the release profile of berberine and rutin-loaded eudragit nanoparticles. There release profile is shown in Fig. 8 (a) berberine release from eudragit nanoparticles, and Fig. 8(b) shows the rutin release profile from

eudragit nanoparticles. It is extremely obvious from the pattern (Fig. 8(a) (b)) shows the eudragit nanoparticle releases berberine and rutin in amounts of 97.56 and 98.35%, respectively, of the drug within 10 hours. As a result, the first 6 hours have seen a 70% release, and then by a prolonged release of the medication (50–55%) over 4 hours, the release increased to 80% in 8 hours. The following criteria can be used to support this release pattern: The prolonged pattern was caused by the progressive degradation of the carrier matrix, and the burst release may have been caused by the drug that was surface-adsorbed. The continuous release pattern is also a function of the drug's slowed own diffusion out from the polymer matrix.

Stability studies of drug-loaded nanoparticles

Stability studies of drug-loaded nanoparticles Table 8 summarizes the physicochemical characteristics of RBE-NPs tested for 90 days under refrigeration. Physical attributes like color and appearance, % drug release, and % of drug content did not change significantly. The findings showed that RBE-NPs should be stored in a refrigerated condition.

Cytotoxicity of nanoparticles

Using the MTT assay, the *in vitro* cytotoxicity activity of RBE-NPs in the EAC cell line was evaluated [Fig. 9]. The treatment of EAC cells with

RBE-NPs at various concentrations reduced the in a dose-dependent manner the cellular function. The RBE-NPs drug has obtained a higher cytotoxic effect. The proportion 83.09 % RBE-NPs was raised to 6.25 µg/ml to promote cell inhibition, after 24-hour incubation. RBE-NPs' respective IC50 value was discovered to be 23.97µg/ml. The outcomes revealed Berberine and rutin secreted from the body have strong cytotoxic effects of artificial NPs on cancer cells. Thus, the above information points to increased specificity of RB from NPs towards the direction of tumors, which is an additional way to enhance therapy out comes and the bioavailability of hydrophobic rutin and berberine.

CONCLUSION

The ionic gelation methods produced eudragit nanoparticles with berberine and rutin loading and showed considerable interaction between the dependent and independent factors Zeta potential, particle size, and it was discovered that encapsulation efficiency was in an acceptable range. There fridge rated state was evident to be an appropriate setting for storing the formulation. The drug release profile *in vitro* has demonstrated maximal and 98 % continuous drugs release after 10 hours. Consequently, it can be said that the medication was loaded. The creation of nanoparticles can be a successful site-specific therapy delivery method for cancer.

REFERENCES

1. Mattiuzzi C, Lippi G. Current cancer epidemiology. *J Epidemiol Glob Health*. 2019; 9(4): 217.
2. Bray F, Ferlay J, Soerjomataram I, Siegel RL, Torre LA, Jemal A. Global cancer statistics 2018: GLOBOCAN estimates of incidence and mortality worldwide for 36 cancers in 185 countries. *CA: A Cancer J Clin*. 2018; 68(6): 394-424.
3. Kashyap D, Tuli HS, Yerer MB, Sharma A, Sak K, Srivastava S et al. Natural product-based nano formulations for cancer therapy: Opportunities and challenges. In *Seminars in Cancer Biology 2021*; 69: 5-23.
4. Wu S, Powers S, Zhu W, Hannun YA. Substantial contribution of extrinsic risk factors to cancer development. *Nature*. 2016; 529 (7584):43-7.
5. Akhlaghi M, Ebrahimpour M, Ansari K, Parnian F, Zarezadeh Mehrizi M, Taebpour M. Synthesis, study and characterization of nano niosomal system containing Glycrriz-haglabra extract in order to improve its therapeutic effects. *Cell Mol Biol*. 2021; 11 (42): 65-82.
6. Mirhosseini M, Shekari-Far A, Hakimian F, Haghirsadat BF, Fatemi SK, Dashtestani F. Core-shell Au@Co-Fe hybrid nanoparticles as peroxide semimimetic nanozyme for antibacterial application. *Process Biochem*. 2020; 95: 131-8.
7. Khatibi SA, Misaghi A, Moosavy MH, Basti AA, Koohi MK, Khosravi P et al. Encapsulation of Zataria multiflora Bioss. essential oil into nanoliposomes and *in vitro* antibacterial activity against Escherichia coli O157: H7. *J Food Process Preserv*. 2017; 41(3): e12955.
8. Omidi M, Malakoutian MA, Choolaei M, Oroojalian F, Haghirsadat F, Yazdian F. A Label-Free detection of bio molecules using micro mechanical biosensors. *Chin Phys Lett*. 2013; 30(6): 068701.
9. Jebelli A, Oroojalian F, Fathi F, Mokhtarzadeh A, de la Guardia M. Recent advances in surface plasmon resonance biosensors for micro RNAs detection. *Biosens Bioelectron*. 2020; 169: 112599.
10. Wanigasekara J, Witharana C. Applications of nanotechnology in drug delivery and design - an insight. *Curr Trends Biotechnol Pharm*. 2016; 10(1): 78-91.
11. Rahimizadeh M, Eshghi H, Shiri A, Ghadamyari Z, Matin MM, Oroojalian F, et al. Fe(HSO₄)₃ as an efficient catalyst for diazotization and diazo coupling reactions. *J Korean Chem Soc*. 2012; 56(6): 716-9.
12. Anselmo AC, Mitragotri S. Nanoparticles in the clinic. *Bioeng Translation Med*. 2016; 1(1): 10-29.
13. Kumari A, Yadav SK, Yadav SC. Biodegradable polymeric nanoparticles based drug delivery systems. *Colloids Surf B Biointerfac*. 2010; 75(1): 1-8.
14. Guerrero-Cázares H, Tzeng SY, Young NP, Abutaleb AO, Quiñones-Hinojosa A, Green JJ. Biodegradable polymeric nanoparticles show high efficacy and specificity at DNA delivery to human glioblastoma *in vitro* and *in vivo*. *ACS nano*. 2014; 8(5): 5141-53.
15. Mujtaba MA, Hassan KA, Imran M. Chitosan-alginate nanoparticles as a novel drug delivery system for rutin. *Int J Adv Biotechnol Res*. 2018; 9: 1895-903.
16. Aqil F, Munagala R, Jeyabalan J, Vadhanam MV. Bioavailability of phytochemicals and its enhancement by drug delivery systems. *Cancer Lett*. 2013; 334(1): 133-41.

17. Khazir J, Mir BA, Pilcher L, Riley DL. Role of plants in anticancer drug discovery. *Phytochem Lett.* 2014;7:173-81.
18. Liu H, Lu H, Liao L, Zhang X, Gong T, Zhang Z. Lipid nano particles loaded with 7-ethyl-10-hydroxycamptothecin-phospholipid complex: invitro and invivo studies. *Drug Deliv.* 2015; 22(6):701-9.
19. Smitha KT, Anitha A, Furuike T, Tamura H, Nair SV, Jaya kumar R. In vitro evaluation of paclitaxel loaded amorphous chitin nano particles for colon cancer drug delivery. *Colloids Surf B Biointerfac.* 2013;104:245-53.
20. Wang S, Chen T, Chen R, Hu Y, Chen M, Wang Y. Emodin loaded solid lipid nano particles: preparation, characterization and antitumor activity studies. *Int J Pharm.* 2012; 430(1-2):238-46.
21. Chou CW, Batnyam O, Hung HS, Harn HJ, Lee WF, Lin HR, Chung JG, Shih YC, Yen SY, Kuo YH, Tsao MH. Highly bio available anti cancer herbal-loaded nano carriers for use against breast and colon cancer invitro and invivo systems. *Polym Chem.* 2013; 4(6): 2040-52.
22. Mudshinge SR, Deore AB, Patil S, Bhalgat CM. Nano particles: emerging carriers for drug delivery. *Saudi Pharm J.* 201;19(3):129-41.
23. Gird CE, DUȚULE, Costea T, Nencu I, Popescu ML, Balaci TD, TUDORELO. Research regarding obtaining herbal extracts with antitumor activity. Note ii. Phytochemical analysis, antioxidant activity and cytotoxic effects of *Chelidonium Majus L.*, *Medicago Sativa L.* And *Berberis Vulgaris L.* Dry extracts. *Chelidonium Majus.* 2017; 2017: 703-8.
24. Pandey A, Vishnoi K, Mahata S, Tripathi SC, Misra SP, Misra V, Mehrotra R, Dwivedi M, Bharti AC. Berberine and curcumin target survivin and STAT3 in gastric cancer cells and synergize actions of standard chemo-therapeutic 5-fluorouracil. *Nutr Cancer.* 2015 Nov 17;67(8):1295-306.
25. Mukerjee A, Vishwanatha JK. Formulation, characterization and evaluation of curcumin-loaded PLGA nano spheres for cancer therapy. *Anticancer Res.* 2009; 29(10): 3867-75.
26. Anwer MK, Al-Shdefat R, Ezzeldin E, Alshahrani SM, Alshetaili AS, Iqbal M. Preparation, evaluation and bioavailability studies of eudragit coated PLGA nanoparticles for sustained release of eluxadolone for the treatment of irritable bowel syndrome. *Front pharmacol.* 2017; 8: 844.
27. Shaikh MV, Kala M, Nivsarkar M. Formulation and optimization of doxorubicin loaded polymer ic nano particles using Box-Behnken design: ex-vivo stability and in-vitro activity. *Eur J Pharm Sci.* 2017; 100: 262-72.
28. Mongia P, Khatik R, Raj R, Jain N, Pathak AK. pH-Sensitive Eudragit S-100 coated chitosan nanoparticles of 5-aminosalicylic acid for colon delivery. *J Biomater Tissue Eng.* 2014; 4(9):738-43.
29. Krishna Sailaja A, Swati P. Preparation and characterization of sulphasalazine loaded nanoparticles by nano precipitation and ionotropic gelation techniques using various polymers. *Current Nano medicine (Formerly: Recent Patents on Nano medicine).* 2017; 7(2): 125-41.

Table 1. Levels and their variables used in Central Composite design

VARIABLE	LEVELS					
			Units	-1	0	+1
Independent variables	X1	Ratio of polymers	%	100:200	100:100	200:100
	X2	Surfactant concentration	%	0.5	1	1.5
	X3	Volume of Organic phase	%	2.5	5	7.5
Constraints						
Dependent variables	Y1	Particle Size (diameter)	mg	Minimize		
	Y2	Zetapotential	mv	Minimize		
	Y3	EE(rutin)	%	Maximize		
	Y4	EE(berberine)	%	Maximize		

Table 2. A description of experimental trials and observable responses from nanoparticles

Formulation runs	Independent variables			Dependent variables			
	Polymer ratio X1(%)	Concentration of surfactant X2(%)	Volume of organic phase X3(%)	Particle size Y1 (mg)	Zeta potential Y2 (mv)	Encapsulation efficacy (berberine) Y 3(%)	Encapsulation efficacy (rutin) Y 4(%)
1	10	10	75	369	-2.3	51	59
2	2	2.5	75	194	-2.1	79	81
3	10	2.5	75	428	-0.82	71	73
4	6	6.25	75	98	-1.2	91	96
5	6	6.25	75	98	-1.2	91	96
6	2	10	75	263	-0.35	49	87
7	6	6.25	75	98	-1.2	91	96
8	6	10	50	406	-3.9	82	86
9	10	6.25	100	263	-4.2	62	65
10	6	6.25	75	98	-1.2	91	96
11	2	6.25	50	175	-2.8	86	82
12	6	6.25	75	98	-1.2	91	96
13	6	10	100	122	-2.2	99	82
14	6	2.5	100	146	-0.96	86	98
15	2	6.25	100	121	-0.82	56	82
16	6	2.5	50	263	-1.3	98	50
17	10	6.25	50	369	-3.9	42	69

Table 3. ANOVA for a quadratic particle size model (response Y1)

Source	Sum of squares	df	Mean squares	F-value	p-value	
Model	2.201E+05	9	24450.48	19.57	0.0004	significant
A-A Eudragit	57122.00	1	57122.00	45.71	0.0003	
B-B Surfactant(PVA)	2080.13	1	2080.13	1.66	0.2380	
C-C Organic Phase	39340.13	1	39340.13	31.48	0.0008	
AB	4096.00	1	4096.00	3.28	0.1131	
AC	676.00	1	676.00	0.5410	0.4859	
BC	6972.25	1	6972.25	5.58	0.0502	
A ²	47869.01	1	47869.01	38.31	0.0004	
B ²	49910.59	1	49910.59	39.94	0.0004	
C ²	3155.33	1	3155.33	2.53	0.1561	
Residual	8747.25	7	1249.61			
Lack off it	8747.25	3	2915.75			
Pure error	0.0000	4	0.0000			
Cor total	2.288E+05	16				

Table 4. Summary of various quadratic parameters

Response	AdjustedR ²	PredictedR ²	Sequential P-value
Particle size(Y1)	0.9126	0.3883	0.0002
Zetapotential (Y2)	0.6047	-1.7672	0.0433
EE of berberine	0.8197	-0.2620	0.0009
EE of rutin	0.7351	-0.8540	0.0096

Table No.5 ANOVA for the model of the quadratic zeta potential (response Y2)

Sources	Sum of squares	df	Mean square	F-value	p-value	
Models	18.85	9	2.09	3.72	0.0486	significant
A-A Eudragit	3.32	1	3.32	5.89	0.0457	
B-B Surfactant(PVA)	1.59	1	1.59	2.83	0.1365	

C-C Organic Phase	1.73	1	1.73	3.07	0.1231	
AB	2.61	1	2.61	4.63	0.0684	
AC	1.30	1	1.30	2.31	0.1725	
BC	0.4624	1	0.4624	0.8211	0.3950	
A ²	1.12	1	1.12	1.99	0.2009	
B ²	0.4413	1	0.4413	0.7836	0.4054	
C ²	6.20	1	6.20	11.01	0.0128	
Residual	3.94	7	0.5632			
Lack of fit	3.94	3	1.31			
Pure error	0.0000	4	0.0000			
Cor total	22.79	16				

Table 6 ANOVA for a quadratic model of berberine encapsulation effectiveness (Response Y3)

Sources	Sum of squares	df	Mean squares	F-value	p-value	
Models	5047.87	9	560.87	9.08	0.0041	significant
A-A Eudragit	242.00	1	242.00	3.92	0.0882	
B-B Surfactant(PVA)	351.12	1	351.12	5.69	0.0486	
C-C Organic Phase	3.13	1	3.13	0.0506	0.8284	
AB	25.00	1	25.00	0.4049	0.5448	
AC	625.00	1	625.00	10.12	0.0155	
BC	210.25	1	210.25	3.40	0.1075	
A ²	3571.64	1	3571.64	57.84	0.0001	
B ²	1.64	1	1.64	0.0266	0.8750	
C ²	0.5921	1	0.5921	0.0096	0.9247	
Residual	432.25	7	61.75			
Lack off it	432.25	3	144.08			
Pure error	0.0000	4	0.0000			
Cor total	5480.12	16				

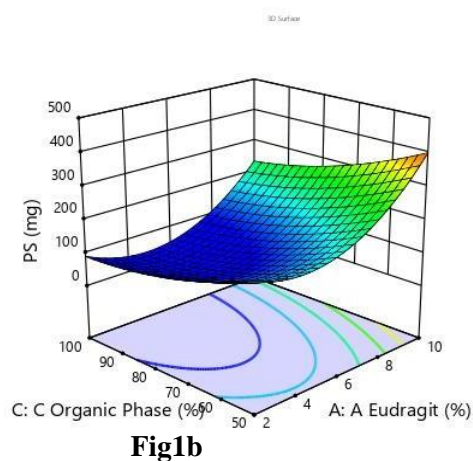
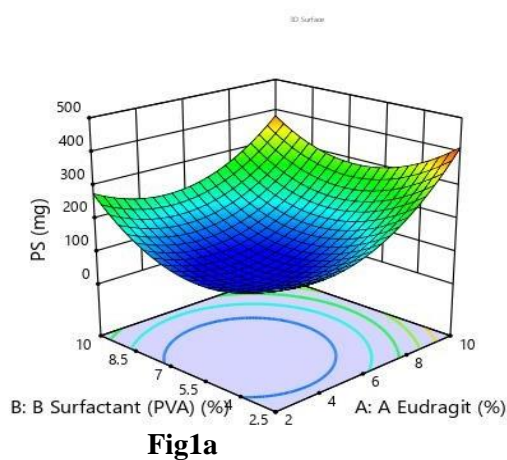
Table No. 7 ANOVA for a quadratic model of rutin's encapsulation effectiveness (Response Y4)

Sources	Sum of squares	df	Mean squares	F-value	p-value	
Models	5047.87	9	560.87	9.08	0.0041	significant
A-A Eudragit	242.00	1	242.00	3.92	0.0882	
B-B Surfactant (PVA)	351.12	1	351.12	5.69	0.0486	
C-C Organic Phase	3.13	1	3.13	0.0506	0.8284	
AB	25.00	1	25.00	0.4049	0.5448	
AC	625.00	1	625.00	10.12	0.0155	
BC	210.25	1	210.25	3.40	0.1075	
A ²	3571.64	1	3571.64	57.84	0.0001	
B ²	1.64	1	1.64	0.0266	0.8750	
C ²	0.5921	1	0.5921	0.0096	0.9247	
Residual	432.25	7	61.75			
Lack of fit	432.25	3	144.08			
Pure error	0.0000	4	0.0000			
Cor total	5480.12	16				
AB	100.00	1	100.00	1.79	0.2225	
AC	4.00	1	4.00	0.0717	0.7966	
BC	676.00	1	676.00	12.12	0.0103	
A ²	684.47	1	684.47	12.27	0.0100	
B ²	286.58	1	286.58	5.14	0.0578	

C ²	322.37	1	322.37	5.78	0.0472	
Residual	390.50	7	55.79			
Lack off it	390.50	3	130.17			
Pure error	0.0000	4	0.0000			
Cor total	3370.00	16				

Table 8. Summary of stability study results under different storage conditions

Drugs	Parameters	Days		
		After 30 days	After 60 days	After 90 days
Berberine	Color and appearance	No change	No change	No change
	% Drug content	96.81±2.14	95.53±1.72	94.11±1.53
	% Drug release	94.52±2.07	94.37±1.43	92.98±1.76
Rutin	Color and appearance	No change	No change	No change
	% Drug content	99.65±1.97	98.63±1.38	97.49±2.01
	% Drug release	98.32±1.09	97.21±1.65	96.92±2.07



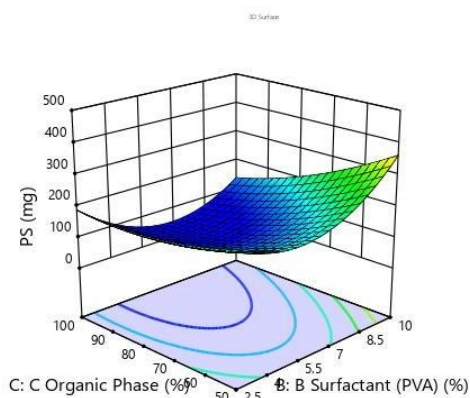


Fig1c

Fig 1. RB-E-Nps3-dimensional Surface Response Plots Demonstrating the Effect of(A) concentration of surfactant and eudragit, (B) Volume of organic and eudragit(C) volume of the organic phase and Concentration of Surfactant

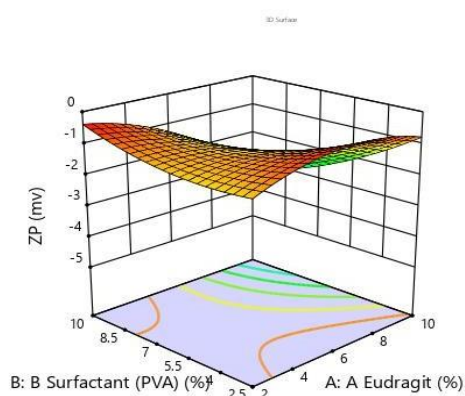


Fig2a

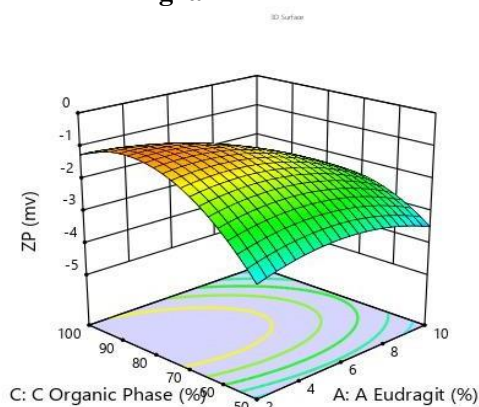


Fig2b

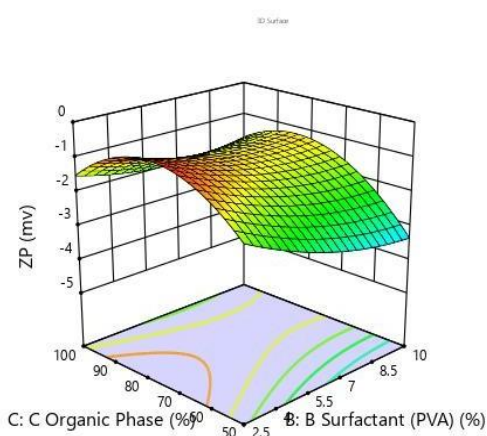


Fig2c

Fig 2. RB-E-Nps3-dimensional Surface Response Plots Demonstrating the Effect of (A) concentration of surfactant and eudragit, (B) Volume of organic and eudragit(C)volume of the organic phase and Concentration of Surfactant

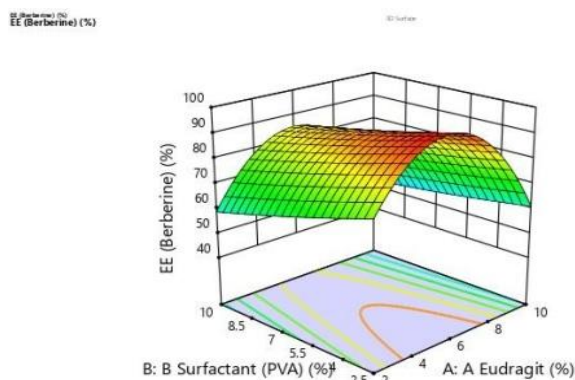


Fig 3a

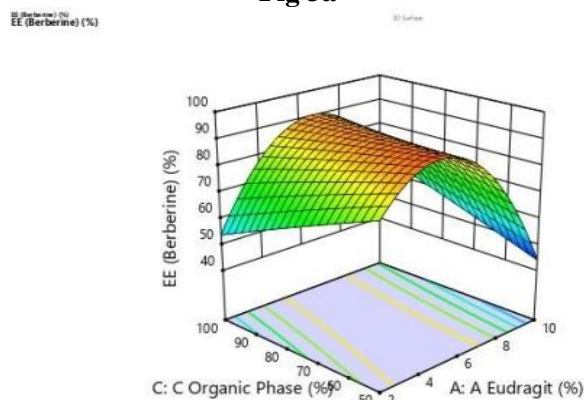


Fig 3b

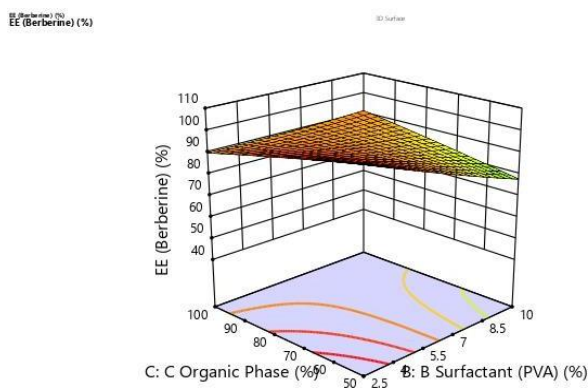


Fig 3c

Fig.3. RB-E-Nps3-dimensional Surface Response Plots Demonstrating the Effect of (A)concentration of surfactant and eudragit, (B) Volume of organic and eudragit(C)volume of the organic phase and Concentration of Surfactant

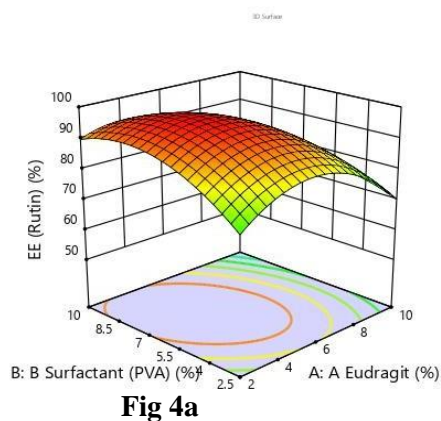


Fig 4a

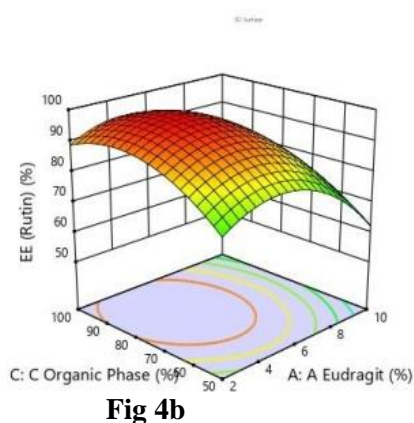


Fig 4b

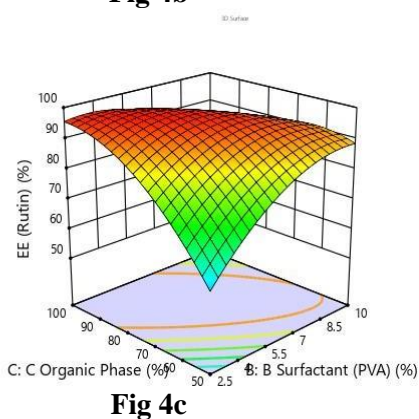


Fig 4c

Fig 4: Three Dimensional Response Surface Plots for RB-E-Nps Showing the Effect of (A) concentration of surfactant and eudragit, (B) Volume of organic and eudragit(C) volume of the organic phase and Concentration of Surfactant

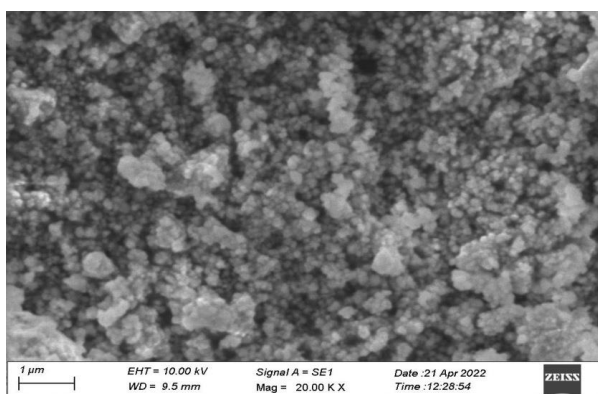


Fig 5. SEM Image of RB-ENPs

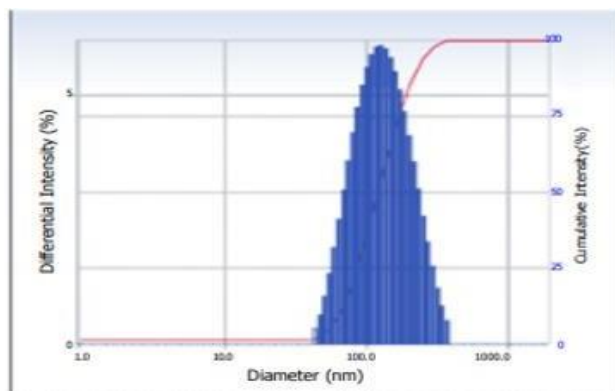


Fig 6. Dispersion of Particle Size of RB-ENPs

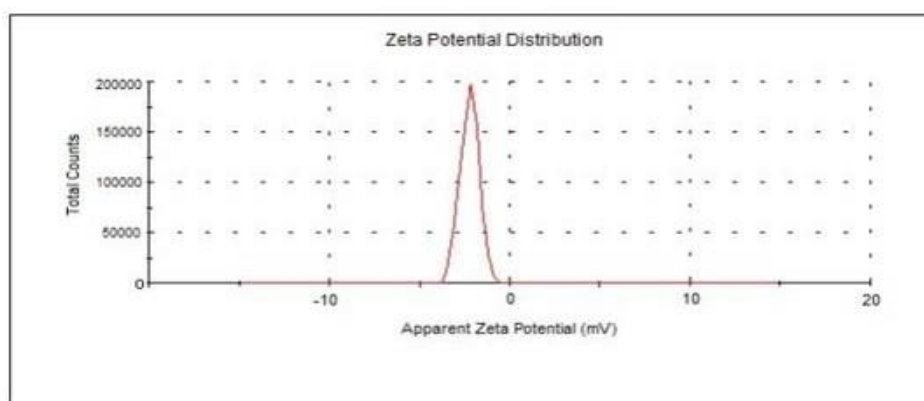


Fig 7. Zeta potential of RB-ENPs (n=3)

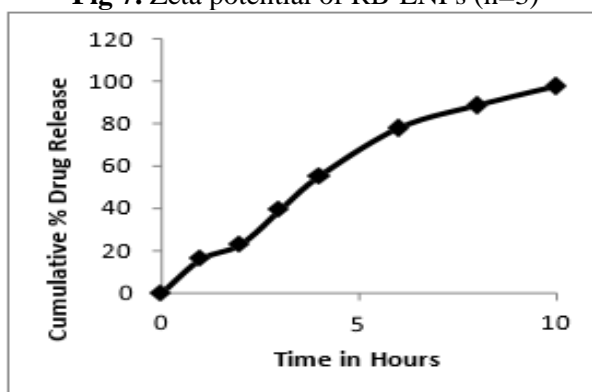


Fig.8 (a) Drug Release in-vitro Study of Nanoparticles with Berberine Loaded,

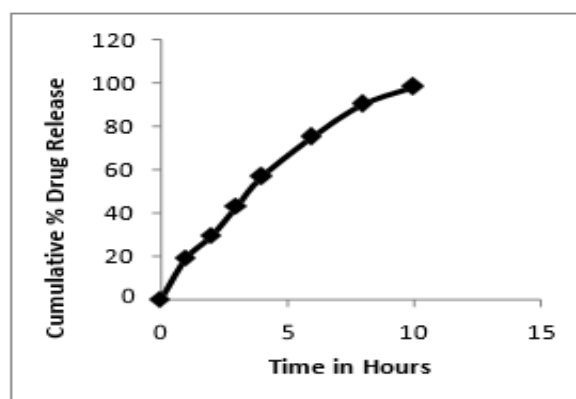


Figure 8(b) Drug Release in Vitro Study of Nanoparticles with Rutin Loaded.

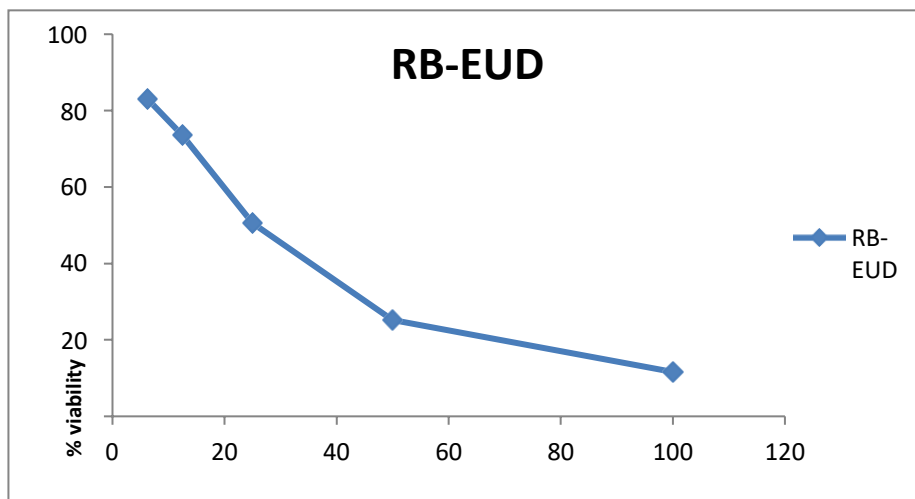
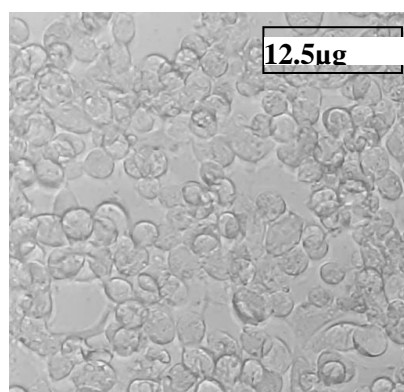
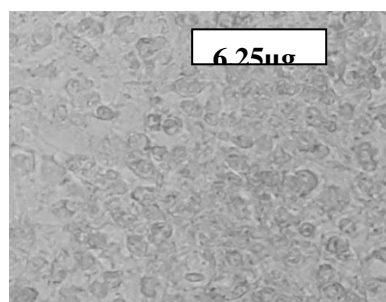
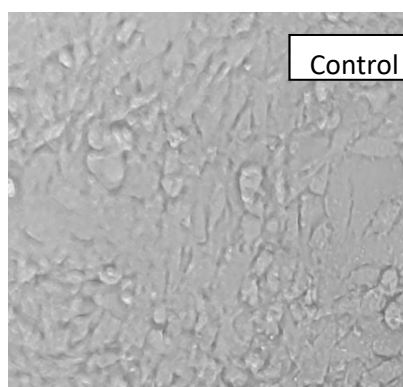


Fig 9. %Cell viability activity of RBE-NPs



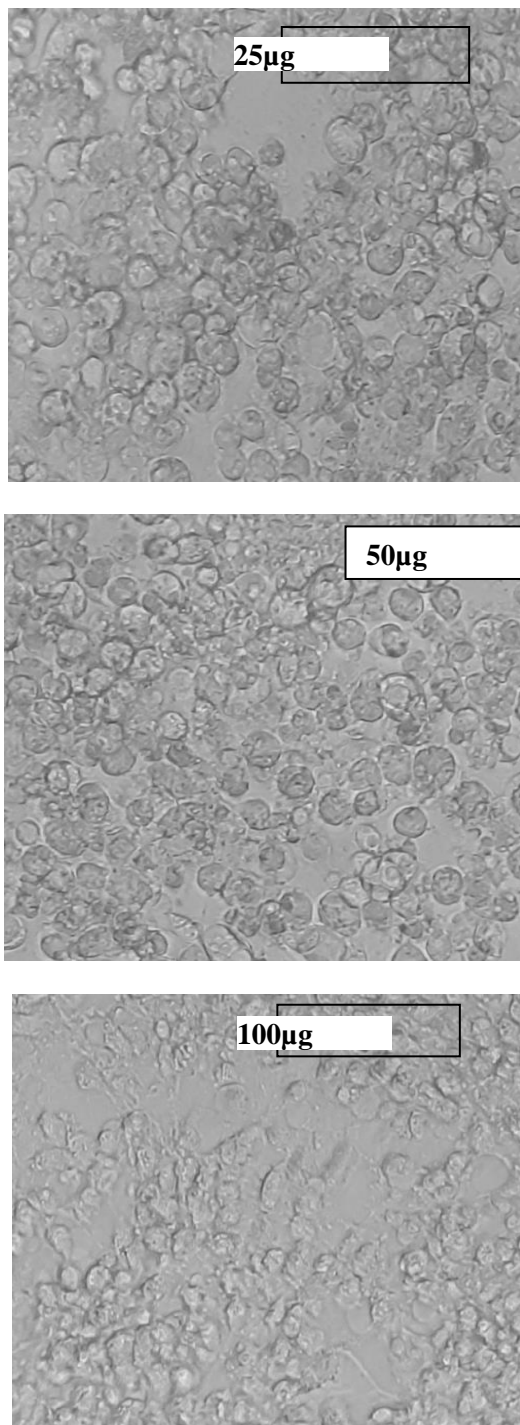


Fig 10. In-vitro cytotoxicity activity of RBE-NPs